Astron. Astrophys. 274, 993–1001 (1993)

ASTRONOMY AND ASTROPHYSICS

Polarized resonance line transfer with collisional redistribution

D. Mohan Rao and K.E. Rangarajan

Indian Institute of Astrophysics Bangalore - 560 034, India

Received October 14, 1992; accepted February 8, 1993

Abstract. In this paper we study the effect of depolarizing collisions on resonance line polarization in the absence of magnetic fields. The role of γ, the coherence parameter is investigated in determining the percentage of polarization across the spectral line profiles. We also try to find out whether the partial frequency redistribution function R_{III} (which describes the frequency redistribution due to collisions) can be replaced by the complete redistribution (CRD, i.e $\phi(x)\phi(x')$) in resonance line polarization calculations. We have chosen idealized models to illustrate the differences in polarization when CRD, R_{III}, and R_{II} functions are used in the radiative transfer calculations. We considered isothermal, effectively thin and semi-infinite atmospheres. R_{III} function gives different polarization in the Doppler core compared to CRD when depolarizing collisions are neglected, but it gives the same polarization as CRD in the wings in all circumstances. It is proposed that any redistribution function which is different from $\phi(x)\phi(x')$ at certain frequencies is likely to show different polarization compared to CRD at those frequencies even though the total specific intensities may not differ.

We find that the percentage of polarization at the line centre to be a monotonic function of the parameter γ when depolarizing collisions are included in the calculations. This important aspect is absent if the depolarizing collisions are neglected. Therefore one may use this property for diagnostic purposes. The character of the wing polarization is altered when $\gamma = 0.9$ compared to $\gamma = 1.0$ (R_{II} redistribution). Therefore γ is an important parameter while evaluating the wing polarization. We find that CRD may be a good approximation to R_{III} when depolarizing collisions are included in the approximation.

Key words: radiative transfer – polarization – stellar atmospheres

1. Introduction

This paper is concerned with the study of linear polarization of strong resonance lines in the absence of magnetic fields. It is well known that some part of elastic collisions depolarize the radiation. Thus it is important to study this process quantitatively. This problem is considered in some detail in this paper. We also investigate the validity of the assumption of replacing the redistribution $R_{III}(x', x)$ function by the complete redistribution function $\phi(x)\phi(x')$, where $\phi(x)$ is the absorption profile function, and the effect of γ, the coherence parameter, on linear polarization results.

1.1. Basic theory

The partial frequency redistribution has been shown to be a viable mechanism for the formation of strong resonance lines in stellar atmospheres (Mihalas 1978; Hubeny 1986). In static plane-parallel atmospheres, the use of angle-averaged redistribution function is a good approximation to the angle-dependent one for the study of polarization as well as intensity profiles. (Milkey et al. 1975; Vardavas 1976; Faurobert 1987, 1988).

Among the redistribution functions derived by Hummer (1962), the angle averaged functions R_{II} and R_{III} have evoked considerable interest. Omont et al. (1972) derived the quantum mechanical form of the redistribution function for resonance lines allowing for the effects of elastic and inelastic collisions. They showed that the atomic frame redistribution function for resonance lines is given by

$$r(x', x) = \gamma\, r_{II}(x', x) + (1 - \gamma) r_{III}(x', x),$$

where γ is the ratio of the atoms that emit coherently to all the atoms in the excited state. The expression for γ is

$$\gamma = \frac{\Gamma_R + \Gamma_I}{\Gamma_R + \Gamma_I + \Gamma_C},$$

where Γ_R, Γ_I and Γ_C are the rates of spontaneous emission, inelastic collision and the elastic collisions respectively. The atomic frame redistribution function $r_{II}(x', x)$ describes the coherent scattering part and $r_{III}(x', x)$, the noncoherent scattering mechanism. They have not considered the angular distribution of the scattered radiation.

Domke & Hubeny (1988) have derived a laboratory frame redistribution matrix for scattering of arbitrarily polarized light by a spatially degenerate atom undergoing collisions. They have included the Stokes vector representation in their derivation.

Send offprint requests to: D. Mohan Rao

Their work closely follows the important works of Omont et al. (1972) and Ballagh & Cooper (1977) and therefore contains the same physical assumptions. Some of them are: 1) Impact parameter approximation to describe the collisions, 2) the initial state of the transition (for resonance transition, the ground state) is isotropic, i.e. unpolarized, 3) Stimulated emission, multilevel phenomena and optical pumping are not present. They obtained the results for $j \rightarrow j \pm 1 \rightarrow j$ atomic transition. Faurobert (1992) has given the expression for source function using the angle averaged redistribution function which was derived by Domke & Hubeny in a convenient form. We use this source function in our calculations. In the next section, we shall describe the observations which are relevant to the partial frequency redistribution formalism.

1.2. Observations pertaining to the theory

Stenflo et al. (1983a,b) have reported a wealth of observations of linear polarization of solar lines. These observations were performed at 10 arcsec inside the solar limb and many of them are yet to be interpreted in detail. The dominant feature is the variation of polarization from line to line which is the interplay between the atomic physics and radiative transfer. The resonance lines Ca I 4227, Ca II H & K, Na I 5890 show non magnetic linear polarization (Stenflo et al. 1980). The observed line polarization shows narrow peak in the Doppler core and maximum in the wings. Henze & Stenflo (1987) have recorded the linear polarization of Mg II h & k lines. Their observations do not show the theoretically predicted negative polarization between the h and k lines. All these observations warrant a detailed study of resonance line polarization formed with partial redistribution mechanism.

1.3. A brief survey of the theoretical calculations of resonance line polarization

Theoretical studies aimed at the interpretation of the linear polarization in resonance lines were made by Rees & Saliba (1982). They employed R_{II} function and showed that this function is responsible for the wing maxima in polarization observed in certain solar lines. To evaluate R_{II} function, they used Kneer's (1975) approximation. In two significant papers, Faurobert (1987, 1988) studied the effect of Kneer's approximation in polarization calculations. She also compared the results of angle-dependent and angle-averaged redistribution functions. She concluded that Ayres (1985) approximation which retains the diffusive behavior of photons in R_{II} function should be used in place of Kneer's approximation and also the angle-averaged function may be used instead of the angle-dependent ones. She obtained some interesting results concerning the effects of ϵ (the probability of the photon being destroyed due to collisions) and β_c, the ratio of continuum to line centre optical depth. Faurobert-Scholl (1991, 1992) has extended her work to include the Hanle effect. In the first paper of this recent series, she replaced R_{III} by $\phi(x)\phi(x')$. In the second paper on Hanle effect, she has done a detailed modelling of Ca I 4227 line and she has used the generalized redistribution function given by Domke & Hubeny (1988) which is a combination of R_{II} and R_{III}. But it is not clear whether she has replaced R_{III} by $\phi(x)\phi(x')$ in her work. She has varied γ throughout the solar atmosphere (γ varies from 10^{-1} to 10^{0} according to the model). In the next section, we briefly outline the existing calculations comparing R_{III} and CRD.

1.4. Differences between R_{III} and CRD

Finn (1967) found that the function R_{III} differs by several orders of magnitude from $\phi(x)\ \phi(x')$ in the Doppler core (Fig. 1. in the quoted paper). He showed that the Doppler motion introduces a correlation between incoming and outgoing frequencies near the line core. He also showed that R_{III} gives larger source functions near the surface of an isothermal semi-infinite atmosphere compared to CRD. However he found that the resulting line profiles from R_{III} do not differ from those of CRD line profiles. The same conclusions about the emergent line intensities was arrived at by Vardavas (1976). When deriving the scaling laws for PRD function ($R_I - R_{IV}$), Frisch (1980) found from asymptotic expressions for R_{III}, that it does not differ from CRD at large frequencies from line center. In the discussion of the effects of stimulated emission on radiative transfer with PRD, Rangarajan et al. (1990) found that R_{III} gives the emission profile same as that of the absorption profile (like CRD) in the line core as well as in the wings, but with a small enhancement at the intermediate points.

2. Polarized line transfer equation and the method of solution

In a non-magnetic plane-parallel atmosphere with azimuthal symmetry in the radiation field, it is sufficient to consider the Stokes parameters I_l and I_r to represent the polarization state of the radiation field. The total intensity is defined as $I = I_l + I_r$ and the Stokes Q parameter is defined as $Q = I_l - I_r$. As in Chandrasekhar (1960), I_l and I_r denote the intensities of linearly polarized radiation along two perpendicular directions l and r. The linear polarization is defined as $p = (Q/I)$. With the above definitions, the vector transfer equation for a two-level atom becomes

$$\mu \frac{d\mathbf{I}(x,\mu,z)}{dz} = -\chi(x,\mu,z)\,\mathbf{I}(x,\mu,z) + \boldsymbol{\eta}(x,\mu,z)\,. \qquad (1)$$

Here $\mathbf{I} = (I_l, I_r)^T$ and $\boldsymbol{\eta}$ is the emission coefficient. The total absorption coefficient is given by

$$\chi(x,\mu,z) = \chi_l(z)\,\phi(x,\mu,z) + \chi_c(x,\mu,z)\,. \qquad (2)$$

The optical depth scale is defined as $d\tau(z) = -\chi_l(z)dz$. The frequency is defined in Doppler units as,

$$x = \frac{\nu - \nu_0}{\Delta\nu_D}, \quad \text{with} \quad \Delta\nu_D = \frac{\nu_0}{c}\sqrt{\frac{2kT}{M}}\,. \qquad (3)$$

In Eq.(2), χ_c and χ_l are the coefficients of continuous absorption and atomic absorption at the line centre respectively. ν_0 is

the line center frequency with $\Delta\nu_D$ as the Doppler width. The velocity of light and Boltzmann constant are denoted by c and k . M is the mass of the atom under consideration. We have used Voigt function as the absorption profile throughout this study. All the other quantities have their usual meaning. The total source function $\mathbf{S}_{tot}(x,\mu,z)$ is given by

$$\mathbf{S}_{tot}(x,\mu,z) = \frac{\phi(x)\mathbf{S_L}(x,\mu,z) + \beta_c \mathbf{S_C}}{\phi(x) + \beta_c}, \quad (4)$$

where $\beta_c = \chi_c/\chi_l$ and continuum source function $\mathbf{S_C}$ is defined as

$$\mathbf{S_C} = \frac{1}{2} B(x)\,\mathbf{1} = \frac{1}{2} B\,\mathbf{1}; \quad \mathbf{1} = \left[1\ 1\right]^T, \quad (5)$$

where B is the Planck function. In the absence of magnetic field, and for the *s-p-s* transition (intrinsic depolarization is absent), Faurobert (1992) gives the following expression for the line source function:

$$\mathbf{S_L}(x,\mu,z) = \frac{(1-\epsilon)}{2\phi(x)} \int_{-\infty}^{+\infty} (\gamma R_{II}(x',x) + bR_{III}(x',x))dx' \times \int_{-1}^{1} \mathbf{P}_R(\mu,\mu')\mathbf{I}(x',\mu',z)d\mu' + \frac{d(1-\epsilon)}{2\phi(x)} \int_{-\infty}^{+\infty} R_{III}(x',x)dx' \times \int_{-1}^{1} \mathbf{P}_{is}\mathbf{I}(x',\mu',z)d\mu' + \frac{\epsilon}{2} B\mathbf{1}, \quad (6)$$

where $\mathbf{P}_R$ is the Rayleigh scattering phase matrix and $\mathbf{P}_{is}$ is the isotropic matrix. The branching ratios b and d are

$$b = \frac{\Gamma_R + \Gamma_I}{\Gamma_R + \Gamma_I + \Gamma_c} \cdot \frac{\Gamma_c - D^{(2)}}{\Gamma_R + \Gamma_I + D^{(2)}} \quad \text{and} \quad d = 1 - \gamma - b, \quad (7)$$

In these expressions, $D^{(2)}$ is the rate of depolarizing elastic collisions and b is the probability that an elastic collision which does not destroy alignment occurs followed by a de-excitation of the atom. Therefore d gives the probability that the elastic collision which destroys alignment occurs followed by a de-excitation of the atom. If there are no depolarizing collisions, $D^{(2)}$ is zero, then $d = 0$ and $b = 1 - \gamma$. $\mathbf{P}_R$ is defined in Chandrasekhar (1960). Using the above expression for the source function and the phase matrices we can also write the line source functions for the Stokes parameters I and Q in the following form:

$$\mathbf{S_L}(x,\mu) = \begin{pmatrix} S_I(x,\mu) \\ S_Q(x,\mu) \end{pmatrix} \quad (8)$$

and

$$S_I(x,\mu) = S_l(x,\mu) + S_r(x,\mu) \quad (9)$$

$$S_Q(x,\mu) = S_l(x,\mu) - S_r(x,\mu) \quad (10)$$

where

$$S_I(x,\mu) = S(x) + (\frac{1}{3} - \mu^2)\bar{P}(x) \quad (11)$$

$$S_Q(x,\mu) = (1-\mu^2)\bar{P}(x) \quad (12)$$

with

$$S(x) = \frac{(1-\epsilon)}{2\phi(x)} \int_{-\infty}^{+\infty} \left[\gamma R_{II}(x',x) + (1-\gamma)R_{III}(x',x)\right]dx' \times \int_{-1}^{+1} I(x',\mu')d\mu' + \epsilon B \quad (13)$$

$$\bar{P}(x) = \frac{3(1-\epsilon)}{8\phi(x)} \int_{-\infty}^{+\infty} (\gamma R_{II}(x',x) + bR_{III}(x',x))dx' \times \tfrac{1}{2}\int_{-1}^{1} \left[(1-3\mu'^2)I(x',\mu') + 3(1-\mu'^2)Q(x',\mu')\right]d\mu' . \quad (14)$$

We have solved Eq. (2) for I_l and I_r. We have considered 27 frequency points in the range[0,80]. Since significant transfer of the radiation takes place in the wings in an optically thick medium, we extended our frequency points up to 80. To find out whether this grid is sufficient, we performed certain calculations (for example $T = 10^8, \epsilon = 10^{-6}$ model) with a grid of [0,250]. We did not find significant difference in the results between these two grids. To reduce the computational time, most of the calculations were performed with [0,80] grid only. The frequency mesh is chosen in [0,3] with an interval of 0.25 and [3,5] at 0.5 interval and [5,80] at larger interval. We found that in the core, one has to choose interval size of 0.25 or less; otherwise errors creep into the polarization calculation. We chose 3 points (Gaussian quadrature points) to represent the angular integration. We have used Ayres (1985) approximation to evaluate R_{II} function. The scattering integral over the atomic redistribution function $R_{II}(x',x)$ is performed by natural cubic-spline representation of the radiation field (Adams et al. 1971).

We modified the Discrete space theory technique of Grant & Hunt (1969) to solve the vector transfer equation. We have checked the percentage of polarization obtained by this method with that of Faurobert (1987,1988) in the following cases where depolarizing collisions were not included 1)$T = 10^2, \epsilon = 10^{-4}$ for R_{II} and CRD functions 2) $T = 10^{12}, \epsilon = 10^{-4}$ for R_{II} and CRD functions and we get good agreement with her results.

3. Results and discussion

We studied separately the resonance polarization for the two cases: Case a). When depolarizing collisions are not present in the medium. This is an idealized case. Case b). The depolarizing collisions are present.

For both the cases, we have considered three types of isothermal homogeneous slabs. One is an effectively thin self-emitting medium with the total line centre optical depth $T = 10^2$ and $\epsilon = 10^{-4}$. When $\Lambda > T$ (Λ is the thermalization length) the medium is said to be effectively thin. For Voigt profile function, $\Lambda \sim a\epsilon^{-2}$. Here the boundary conditions are

$$\mathbf{I}(\tau = T, x, \mu) = 0, \quad \mu \in (0,1). \quad (15)$$

The second is an optically thick medium with $T = 10^8$ and there is incident radiation at the lower boundary

$$\mathbf{I}(\tau = T, x, \mu) = 0.5. \quad (16)$$

In all the cases we have kept the damping parameter $a = 10^{-3}$. The third is semi-infinite atmosphere with $T = 10^{12}$ and an incident radiation at the lower boundary. In the absence of depolarizing collisions, i.e. for the case a) the d term which is defined in Eq. (7) is zero and hence the redistribution function reduces to

$$R(x,x') = \gamma R_{II}(x,x') + (1-\gamma)R_{III}(x,x') \quad (17)$$

or

$$R(x,x') = \gamma R_{II}(x,x') + (1-\gamma)\phi(x)\phi(x'), \quad (18)$$

if R_{III} is approximated to CRD. When $\gamma = 0$, the above redistribution functions reduce to $R_{III}(x,x')$ and CRD ($\phi(x)\phi(x')$) respectively. When $\gamma = 1$, only the R_{II} term remains in the above expressions. For the case b) where depolarizing collisions are present,we have assumed the inelastic collision rate to be negligible compared to the radiative decay, i.e. Γ_I/Γ_R is very small. In this case, $D^{(2)} = 0.379\Gamma_C$ (Faurobert 1992; Ballagh & Cooper 1977). With this approximation we get,

$$b = (1-\gamma)\frac{0.621}{1+0.379\frac{1-\gamma}{\gamma}}. \quad (19)$$

Now all the three integrals in Eq. (6) are present. The third term which multiplies the d coefficient is the isotropic scattering part and this will reduce the polarization. Since this is proportional to $(1-\gamma)$, we expect that the smaller γ values will result in lesser percentage of polarization.

We have plotted the percentage of polarization along the direction $\mu = 0.11$ in the y-axis and frequency x in the x-axis in the top panel of all the figures and Log I (I is the total specific intensity along $\mu = 0.11$) is plotted in the y-axis of the bottom panel. Some authors prefer to plot the Feautrier variable u which is $I/2$, but we have preferred to show the variation of emergent specific intensity $I(\mu = 0.11)$ as a function of frequency. Our starting point in the frequency scale shown in the figures is x=0.25.

3.1. Case a: when depolarizing collisions are not present

3.1.1. Effectively thin medium

In Fig. 1, we have plotted the percentage of polarization in a spectral line where the line centre optical depth T=100, $\epsilon = 10^{-4}$ and β_c=0. The curve 1 (for R_{III} redistribution i.e $\gamma = 0$) shows negative polarization peak at the line centre and reduces as x increases in the Doppler core. But surprisingly it reaches a positive peak (2.8%) in the interval $2 < x < 3$. It reduces at higher frequencies and reaches a constant value of $\sim 0.7\%$ in the wings. The same qualitative behaviour but with different magnitudes is seen for the polarization due to R_{II} partial redistribution (see Faurobert 1987). Polarization seems to be behaving very similar to that of the emission profile calculated by Rangarajan et al. (1990). They performed partial redistribution, radiative transfer calculations assuming that the emission profile is not the same as that of the absorption profile. They found that the emission

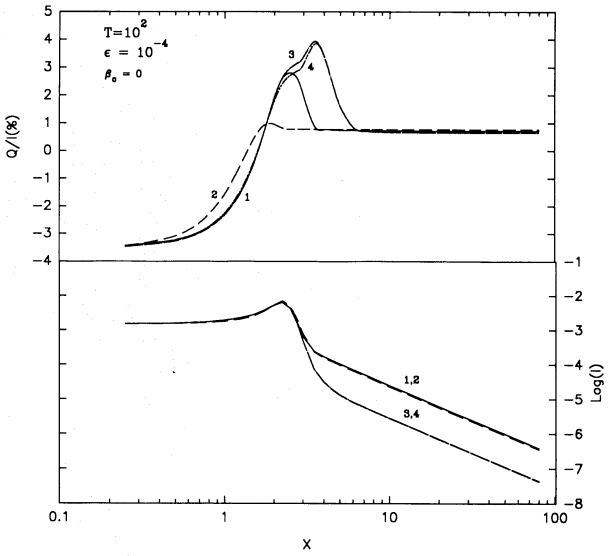

Fig. 1. In the top panel, percentage of polarization in the direction $\mu = 0.11$ is plotted against the frequency x measured from line centre in units of Doppler width. The numbers shown near the curves represent the cases mentioned below: curves 1 and 2 are for $\gamma = 0$ case; i.e., the results for R_{III} and CRD respectively. Curves 3 and 4 are for the coherence parameter $\gamma = 0.9$ case, namely, $R = 0.9R_{II} + 0.1R_{III}$ and $R = 0.9R_{II} + 0.1(CRD)$ respectively. The figure shows the variation of polarization in a spectral line formed in an optically thin ($T = 10^2$) self-emitting slab. The bottom panel shows the variation of the logarithm of emergent specific intensity Log I in the direction $\mu = 0.11$ with respect to the same x-axis as in the top panel for the various cases mentioned above

profile is different from absorption profile for R_{III} in the frequency range $1.0 < x < 3.5$ but same in the wings ($x > 4.0$ as in the case of CRD). Comparing curves 1 and 2 (curve 2 is for CRD), we find a similar pattern. That is the polarization is different for R_{III} and CRD in the above frequency range. This may be interpreted as due to the difference between the functions R_{III} and $\phi(x)\phi(x')$ which is large at those frequencies. These results are worth noting because in future any polarization calculation performed using any other redistribution function (for example R_V which describes the scattering in the subordinate lines) may show different polarization from that of CRD at the frequencies where the function values are very much different from the product $\phi(x)\phi(x')$. It is of an academic interest to plot $R_V(x,x')/\phi(x)\phi(x')$ and also perform the polarization calculations to verify our speculation.

The curves 3 and 4 show the polarization for the case $\gamma = 0.9$. These curves correspond to 90% of R_{II} function mixed with 10% of R_{III} (curve 3) or CRD (curve 4). The curves closely resemble the curves obtained by Faurobert (1987) but with a reduced positive peak (reduced by 2% compared to R_{II} case) in polarization. We also find a small positive percentage of polarization in the wings (0.7%) compared to the zero percentage of polarization in the wings for R_{II}. Therefore we can say that a mixing of 10% of R_{III} or CRD with R_{II} has significant effect

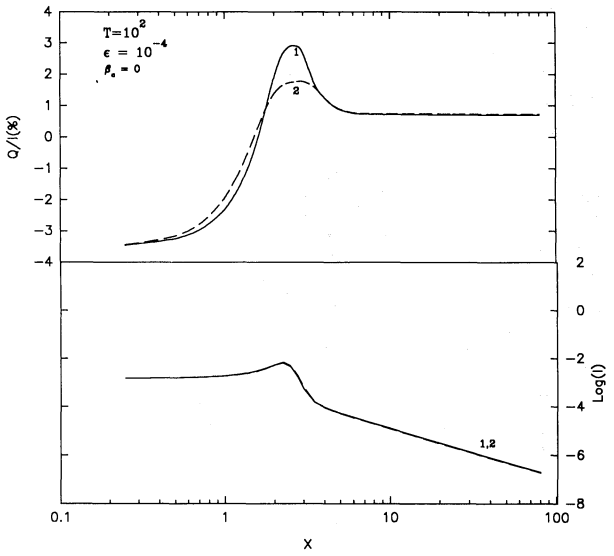

Fig. 2. Curves 1 and 2 are the same as curves 3 and 4 of Fig. 1. but for $\gamma = 0.5$ case

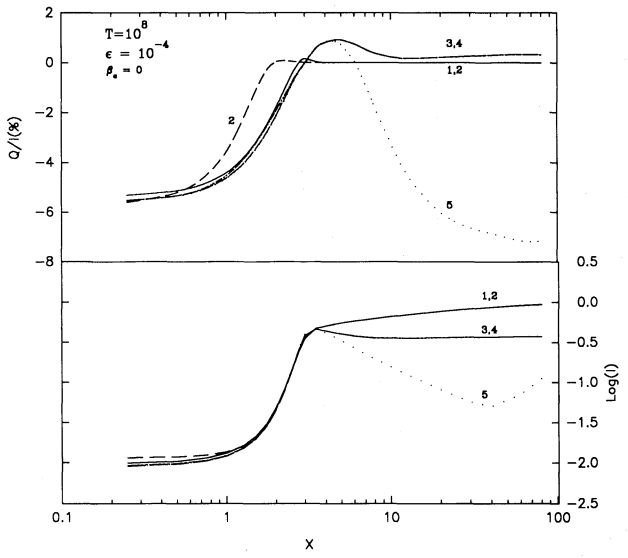

Fig. 3. Same as Fig. 1, but for the optical thickness $T = 10^8$ and now the atmosphere is irradiated at $\tau = T$. Curve 5 represent $\gamma = 1$, namely, R_{II} case

in the percentage of polarization in the frequency range $x > 4.0$ for effectively thin medium.

We have plotted the total emergent specific intensity at $\mu = 0.11$ in the bottom panel. We find that R_{III} and CRD give the same intensity throughout the frequency domain. Since this result is common for the various cases considered, we can conclude that R_{III} can be approximated to CRD if we are interested only in the total specific intensity.

The top panel of the second figure shows the polarization obtained when $\gamma = 0.5$, that is a mixing of 50% of R_{II} function with 50% of either R_{III} (curve 1) or CRD (curve 2). Polarization curve due to $R_{III}+R_{II}$ resembles that of $\gamma = 0$ case (curve 1 of

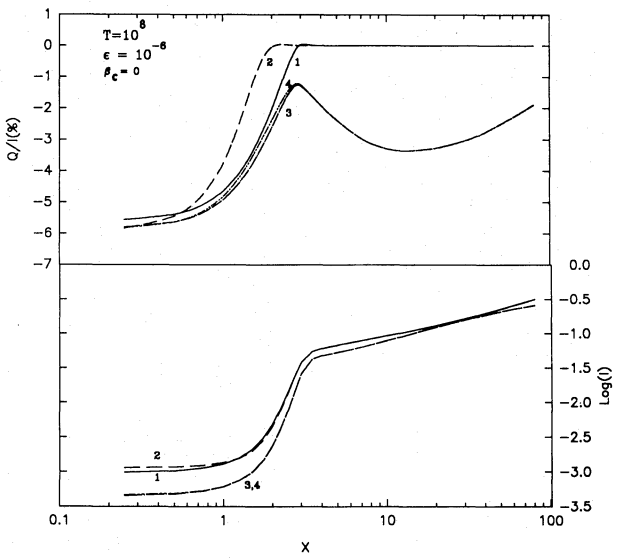

Fig. 4. Same as Fig. 3. but for $\epsilon = 10^{-6}$. There is no corresponding curve 5 here

Fig. 1). For CRD+R_{II} case, the curve 2 shows a small positive peak at $x \sim 2.5(\sim 2\%)$.

3.1.2. Optically thick medium

Figure 3 shows the polarization behaviour in an optically thick medium ($T = 10^8, \epsilon = 10^{-4}$, for $\gamma = 0.0$ and 0.9 and incident radiation at one of the boundaries). The curves 1 and 2 show the R_{III} and CRD results and 3 and 4 are the results for the mixture of R_{II} and R_{III} and R_{II} and CRD respectively. The curve 5 represents the R_{II} case ($\gamma = 1.0$). We find significant difference (nearly 1.5%) in polarization between R_{III} and CRD in the core. For $\gamma = 0$, the polarization in the wings is zero whereas for $\gamma = 0.9$, we get polarization around 0.3% which is not very significant. The difference between R_{III} and CRD in the core has been explained in the previous paragraphs. For an optically thick medium, R_{II}, ($\gamma = 1.0$, curve 5) gives a narrow polarization peak near the line centre and a wing maxima ($\sim -7\%$)(see also Nagendra et al. 1992). But now mixing R_{II} with 10% of R_{III} or CRD removes the maxima in the wings (curves 3 and 4). We have performed the calculations for various γ in between 0.9 and 1.0 and they show a smooth variation from high percentage values for γ=1.0 to nearly zero percent for $\gamma = 0.9$. One such case of $\gamma = 0.98$ when depolarizing collisions are present is plotted in Fig. 8 and discussed in Sect. 3.2.2. This shows that the polarization in the wings is very sensitive to the collisional rate for optically thick lines in finite atmospheres.

The effect of the thermalization parameter ϵ is studied for an optically thick ($T = 10^8$) medium in Fig. 4. Again curves 1 and 2 represent $\gamma = 0.0$ and curves 3 and 4 represent $\gamma = 0.9$ cases. Now the difference between R_{III} and CRD in the core is higher compared to $\epsilon = 10^{-4}$ cases. In the wing, they give identical results. For $\gamma = 0.9$, unlike as in the case of $\epsilon = 10^{-4}$, we find a secondary maximum of polarization in the wings($\sim -3.5\%$).

Table 1. The percentages of polarization Q/I% at various frequencies (x) in the line are shown for different values of γ. The results are for a semi-infinite medium ($T = 10^{12}, \epsilon = 10^{-4}, \beta_c = 0$) without depolarizing collisions. A comparison is made for R_{II} and R_{III} combination (shown as R_{III}) and R_{II} and CRD combination (shown as CRD).

x	$\gamma = 0.9$		$\gamma = 0.5$		$\gamma = 0.2$		$\gamma = 0.0$	
	R_{III}	CRD	R_{III}	CRD	R_{III}	CRD	R_{III}	CRD
0.0	-5.58	-5.61	-5.48	-5.66	-5.41	-5.70	-5.37	-5.73
1.0	-4.64	-4.55	-4.54	-4.08	-4.47	-3.77	-4.43	-3.58
2.5	-0.86	-0.79	-0.66	-0.34	-0.54	-0.09	-0.47	0.20
5.0	0.91	0.91	0.59	0.59	0.22	0.20	0.0	0.0
80.0	0.35	0.35	0.99	0.99	0.40	0.40	0.0	0.0

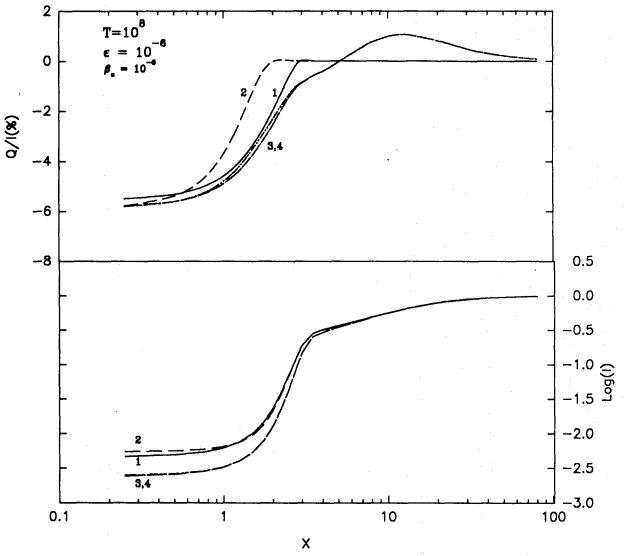

Fig. 5. Same as Fig. 4 but the effect of continuous opacity ($\beta_c = 10^{-6}$)

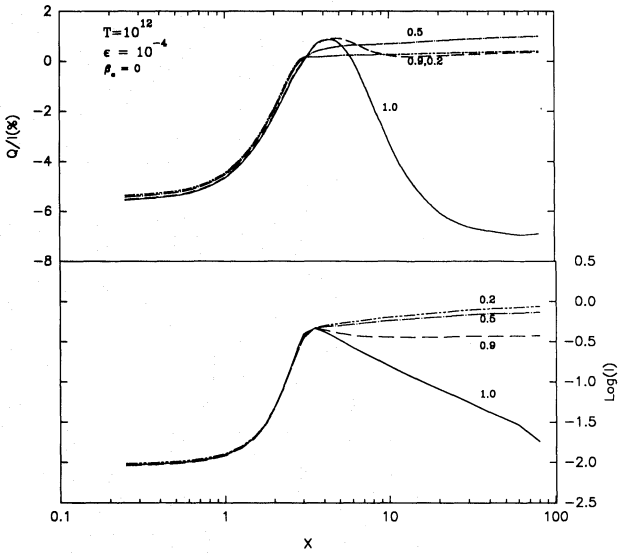

Fig. 6. In the top panel, the percentage of polarization in the direction $\mu = 0.11$ is plotted against the frequency x for various values of γ for a semi-infinite atmosphere ($T = 10^{12}, \epsilon = 10^{-4}$ which is irradiated at $\tau = T$). The γ values are shown near the curves. These results represent the case of R_{II} and R_{III} combination in the scattering integral. The bottom panel shows the corresponding intensity values. $\gamma = 1.0$ corresponds to R_{II} alone

We also find that this secondary maximum reduces when γ is reduced. For example, $\gamma = 0.5$ shows a secondary maximum of $\sim -1.5\%$ in the wings. It appears that R_{II} gives significant contribution in the wings unlike the earlier cases where CRD is dominating the wing polarization.

In Fig. 5, we study the effect of continuous opacity ($\beta_c = 10^{-6}$) for $\gamma = 0.9$ and $\epsilon = 10^{-6}$. We find that the secondary negative maximum in polarization encountered in the wings is replaced (compare curves 3 and 4 of Fig. 4.) with a small positive peak and zero polarization in the far wings.

3.1.3. Semi-infinite atmosphere

Figure 6 shows the results for a semi-infinite atmosphere ($T = 10^{12}, \epsilon = 10^{-4}, \beta_c = 0$) for various values of γ for the case of R_{II}, R_{III} combination. We find that for $\gamma = 1.0$ (R_{II}) our results of percentage of polarization coincides with that of Faurobert (1988). These results are similar to the results for optically thick medium ($T = 10^8, \epsilon = 10^{-4}$, see Fig. 3.). The important point to be noted from this Fig. 6 is that for various values of γ, at the line center we get approximately the same percentage of polarization. This can be explained as follows: The elastic collisions are included through $(1-\gamma)R_{III}$ function. Since R_{II} and R_{III} functions give fairly similar polarization profiles in the line core, the γ parameter does not alter the core polarization. Table 1 gives the comparison between the polarization results at various frequencies when R_{II} and R_{III} combination and R_{II} and CRD combinations are used in the calculations. From this table we observe the following points. In the Doppler core, we get different percentage of polarization when R_{II} and CRD combination is used compared to R_{II} and R_{III} combination. These differences are enhanced for the lower values of γ; i.e. when the collisional rates become important or in other words the contribution from R_{II} function decreases. The same effect has been noted for effectively thin media and optically thick media in Figs. 1-3.

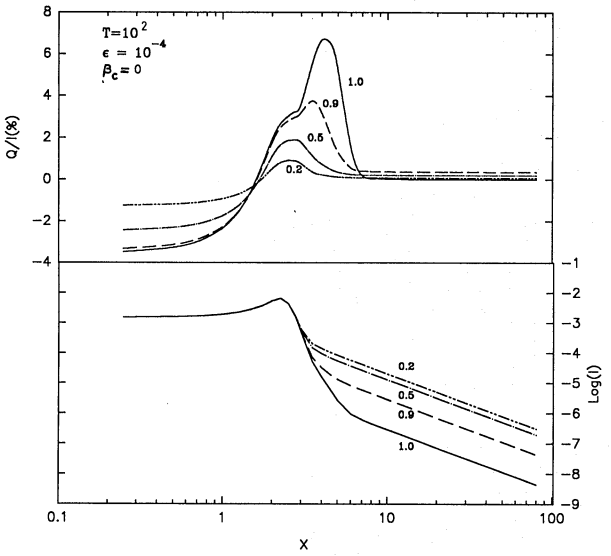

Fig. 7. The top panel results show the effect of depolarizing collisions on the percentage of polarization for various values of coherence parameter γ for an effectively thin ($T = 10^2, \epsilon = 10^{-4}, \beta_c = 0$) self emitting medium. The bottom panel shows the corresponding specific intensity values

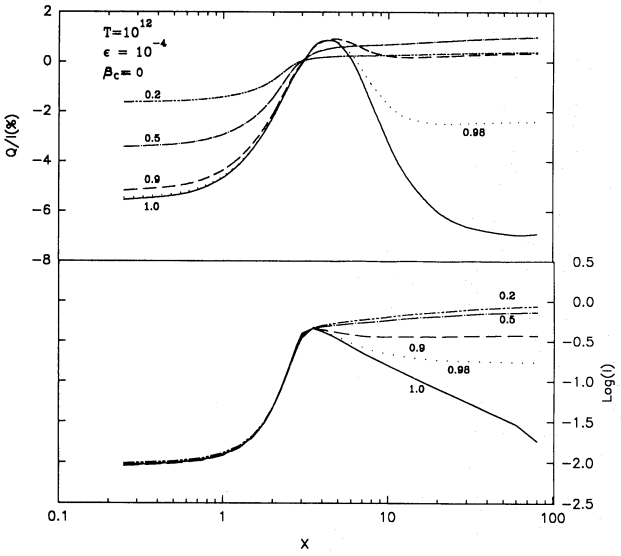

Fig. 8. The same as Fig. 7 but for a semi-infinite atmosphere which is irradiated at $\tau = T$

Table 2. Same as Table 1. but for an optically thin self emitting slab ($T = 10^2, \epsilon = 10^{-4}, \beta_c = 0$) with depolarizing collisions.

x	$\gamma = 0.9$		$\gamma = 0.5$		$\gamma = 0.2$	
	R_{III}	CRD	R_{III}	CRD	R_{III}	CRD
0.0	-3.40	-3.37	-2.47	-2.41	-1.26	-1.23
1.0	-2.27	-2.21	-1.74	-1.54	-0.92	-0.76
2.5	2.79	2.62	1.86	1.30	0.91	0.48
5.0	1.33	1.33	0.35	0.36	0.12	0.12
80.0	0.36	0.36	0.20	0.20	0.08	0.08

Table 3. Same as Table 2. but for a semi-infinite atmosphere ($T = 10^{12}, \epsilon = 10^{-4}, \beta_c = 0$) with depolarizing collisions.

x	$\gamma = 0.9$		$\gamma = 0.5$		$\gamma = 0.2$	
	R_{III}	CRD	R_{III}	CRD	R_{III}	CRD
0.0	-5.23	-5.20	-3.46	-3.42	-1.64	-1.64
1.0	-4.37	-4.30	-2.93	-2.69	-1.42	-1.23
2.5	-0.84	-0.79	-0.50	-0.36	-0.24	-0.13
5.0	0.91	0.90	0.59	0.59	0.22	0.22
80.0	0.35	0.35	0.99	0.99	0.40	0.40

3.2. Case b: when depolarizing collisions are present

Now the depolarizing collisions are included through the parameter d. To calculate this parameter, one should know $D^{(2)}$. When Γ_I/Γ_R is small, $D^{(2)} = 0.379\Gamma_C$ (see Berman & Lamb 1969; Ballagh & Cooper 1977). This approximation may be valid for strong resonance lines. With this value of $D^{(2)}$, we get $d = 0.04, 0.275$ and 0.6 when $\gamma = 0.9, 0.5$ and 0.2. We have performed the calculations using the above set of values of γ. We have considered two types of media; 1) effectively thin medium, and 2) semi-infinite medium.

3.2.1. Effectively thin medium

The boundary conditions and the physical parameters considered are the same as that mentioned earlier. We have shown the effect of depolarizing collisions on the percentage of polarization for an effectively thin, self emitting medium for various values of the coherence parameter γ in Fig. 7 (which gives the results for R_{II} and R_{III} combination). From this figure we discern certain pattern which is described below:- 1) The percentage of polarization at the core is reduced when the coherence parameter γ is reduced. From Eq. (7), we can see that when γ is reduced, the depolarizing collision parameter d is increased. Hence the percent of polarization at the core is decreased. The result is physically consistent and self explanatory. 2) The decrease in the core polarization is more than a factor of 2 from $\gamma = 0.9$ to 0.2. 3) The positive peak at the intermediate frequency points also get reduced and the frequency at which the peak occurs gets shifted towards the line centre when γ is reduced from 1.0 to 0.2. 4) In the wing, a frequency independent, negligible (close to zero) percentage of polarization is obtained. These facts may be used for diagnostic purposes. Table 2 gives the difference in polarization when R_{III} redistribution is used compared to CRD approximation. We find that there is very little difference in polarization at the core and the wing when the two different scattering functions are used.But for $\gamma = 0.2$, we find that the percentage of polarization is nearly twice for R_{II}, R_{III} combination compared to R_{II}, CRD combination around $x = 2.5$.

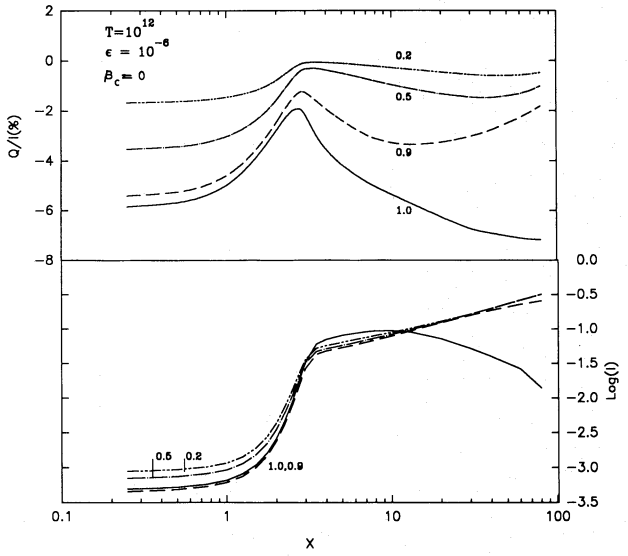

Fig. 9. The same as Fig. 8 but for $\epsilon = 10^{-6}$

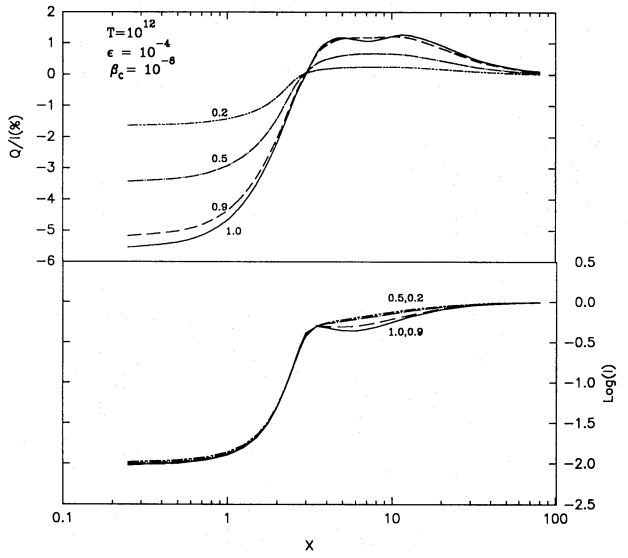

Fig. 10. The same as Fig. 8 but for $\beta_c = 10^{-6}$. That is continuous absorption is included

3.2.2. Semi-infinite atmosphere

We have plotted the percentage of polarization for a semi-infinite atmosphere ($T = 10^{12}, \epsilon = 10^{-4}, \beta_c = 0$) in the top panel of Fig. 8 for various values of γ. Figure 8 gives the results when R_{II} and R_{III} combination is used. We again find the core polarization to be different for different γ's. When $\gamma = 1$, we get high polarization in the wings. This result matches with that of Faurobert (1988). For $\gamma = 0.9$, the wing polarization drastically reduces and is close to zero (only 0.4%). $\gamma = 0.98$ gives intermediate values showing a smooth variation of the percentage of polarization with respect to γ. The wing polarization in Fig. 8 looks very similar to that in Fig. 6. It is not very much affected by depolarizing collisions. We see from the bottom

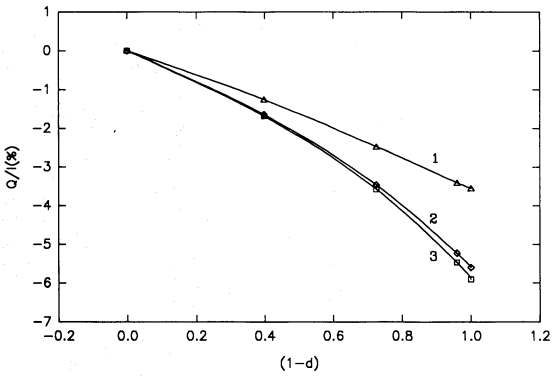

Fig. 11. The percentage of polarization at the line center Q/I% is plotted against $(1-d)$ for various models. Depolarizing collisions are included in all these models. Curve 1 is for $T = 10^2, \epsilon = 10^{-4}$ (effectively thin medium). Curve 2 is for semi-infinite atmosphere with $\epsilon = 10^{-4}$. Curve 3 is the same as curve 2 but for $\epsilon = 10^{-6}$

panel of the figure, the wing intensity is very much different for $\gamma = 0.9$ case compared to $\gamma = 1.0$ case. A similar behaviour is seen for $T = 10^8, \epsilon = 10^{-4}$ (Fig. 3). In the wing R_{II} may be approximated by a coherent (Dirac delta) function and then the contribution from the scattering integral becomes $\sim (1-\epsilon)J(x)$ which is quite small, whereas for CRD or R_{III} we get the scattering integral to be $\frac{(1-\epsilon)}{2}\int_{-\infty}^{+\infty} J(x')\phi(x')dx'$. Therefore there is a contribution from the radiation at all the frequencies to the wing intensity which is quite large. Hence we get an order of magnitude difference in the wing intensity between CRD and R_{II}. To see if CRD gives quantitatively different results from that of R_{III}, we have tabulated the value of percentage of polarization in Table 3 at different frequencies. From this table, we find that R_{II} and R_{III} combination does not give significantly different values for polarization compared to R_{II} and CRD combination at line center and in the wings. As in the case for optically thin atmospheres, for $\gamma = 0.2$, we find that the percentage of polarization for R_{II},R_{III} combination is nearly twice compared to R_{II}, CRD combination around $x = 2.5$.

Figure 9 shows the effect of the thermalization parameter ϵ on polarization. Now ϵ is reduced to 10^{-6} keeping the other parameters same as Fig. 8. We find that the polarization behaves as a monotonic function of $1-d$ at any frequency in the line. Reduction of ϵ reduces the contribution from thermal sources and we get higher percentage of polarization.

The effect of continuous opacity on polarization is shown in Fig. 10. We find the wing polarization is affected by the presence of continuous opacity ($\beta_c = 10^{-6}$). This gives a small positive polarization ($\sim$ 1%) in the near wing, but in the far wing the polarization reduces to zero for all γ's. This figure compares well with Fig. 5 for $T = 10^8$.

The parameter $1-d$ gives the alignment preserving transitions. Therefore, at the line center, this parameter is a sensitive indicator of polarization. So we have plotted Q/I% versus (1-d) in Fig. 11 for various models. We find that the percentage of polarization at the line center is a monotonic function of 1-d but, not linear. This fact may be used for diagnostic purposes.

4. Conclusions

We have investigated the effects of elastic collisions on resonance line polarization profiles, both when depolarizing collisions are neglected and when they are taken into account in an approximate way, following Ballagh & Cooper (1977) (the rate of depolarizing collisions is a constant percentage of the total elastic collision rate). In the first case, the redistribution matrix is proportional to the Rayleigh phase matrix and the frequency redistribution function is the linear combination $\gamma R_{II} + (1-\gamma)R_{III}$. The branching ratio γ measures the fraction of scattering events which are not perturbed by elastic collisions. In the second case, the redistribution matrix is a linear combination of the Rayleigh phase matrix, with the frequency redistribution function $\gamma R_{II} + bR_{III}$, and of the isotropic phase matrix with the frequency redistribution $(1-\gamma-b)R_{III}$. In the approximation of Ballagh and Cooper the parameter b depend on γ only.

We have calculated for different models, the effect on the polarization profiles of varying the parameter γ. We have also looked for the validity, in polarization calculations, of replacing the redistribution function R_{III} by complete frequency redistribution.

For all models used here (isothermal slabs or semi-infinite atmospheres with depth-independent parameters), we find that this approximation allows to recover the polarization rates at line center and in the wings. In the intermediate frequency domain between the line core and wings, around 2 Doppler widths from line center, it leads to significant underestimations of the polarization when γ is smaller than 0.9. These results hold when depolarizing collisions are taken into account.

If elastic depolarizing collisions are neglected, the line core polarization is not sensitive to the value of γ. The reason is that R_{II} and R_{III} give fairly similar polarization profiles in the line core. On the contrary, in the wings they lead to very different behaviours of the polarization profiles. Clearly when the redistribution function is the linear combination $\gamma R_{II} + (1-\gamma)R_{III}$, the wing polarization is very sensitive to the value of γ. We find that when γ decreases from 1 (pure R_{II} regime) to 0 (pure R_{III}), the wing profile is fairly rapidly dominated by the R_{III} regime (as soon as $\gamma < 0.98$ in the case of a semi-infinite atmosphere).

Depolarizing collisions have a drastic effect on the polarization profiles in the line core. When γ decreases, the polarization rate at line center decreases like a monotonic function of $1-d$, where $d = 1-(\gamma+b)$ specifies the fraction of scattering events which are perturbed by depolarizing collisions.

Acknowledgements. We are indebted to the unknown referee who drew our attention to the effect of depolarizing collisions which gave us the opportunity to perform such calculations and for many helpful suggestions which led to a significant improvement of the manuscript. We like to thank Prof.A.Peraiah for the facilities he provided us and also his constant encouragement. We are grateful to Mr. B.A.Varghese for his help in making the figures shown in this paper.

References

Adams J.F., Hummer D.G., Rybicki G.B., 1971, J. Quant. Spectrosc. Radiat. Transfer. 11, 1365
Ayres T.R., 1985, ApJ 294, 153
Ballagh R.J., Cooper J., 1977, ApJ 213, 479
Berman P.R., Lamb W.E., 1969, Phys. Rev. 187, 221
Chandrasekhar S., 1960, Radiative Transfer, Oxford University Press, Dover
Domke H., Hubeny I., 1988, ApJ 334, 527
Faurobert M., 1987, A&A 178, 269
Faurobert M., 1988, A&A 194, 268
Faurobert-Scholl M., 1991, A&A 246, 469
Faurobert-Scholl M., 1992, A&A 258, 521
Finn G., 1967, ApJ 147, 1085
Frisch H., 1980, A&A 83, 166.
Grant I.P., Hunt G.E., 1969, Proc.R.Soc.London A 313, 183
Henze W., Stenflo J.O., 1987, Solar Phys.111, 243
Hubeny, I., 1985, Progress in Stellar Spectral Line Formation Theory In: Beckman J.E., Crivellari L. (eds.) General Aspects of Partial Redistribution and its Astrophysical Importance, Dordrecht:Reidel, p.27
Hummer D.J., 1962, MNRAS 125, 21
Kneer F., 1975, ApJ 200, 367
Mihalas D., 1978, Stellar Atmospheres, 2nd edn., Freeman, San Francisco
Milkey R., Shine., Mihalas D., 1975, ApJ 202, 250
Nagendra K.N., Rangarajan K.E., Mohan Rao D., 1992, MNRAS (accepted)
Omont A., Smith E., Cooper J., 1972, ApJ 175, 185
Rangarajan K.E., Mohan Rao D., Peraiah, A., 1990, A&A 235, 305
Rees D.E., Saliba G., 1982, A&A 115, 1.
Stenflo J.O., Baur T.O., Elmore D.F., 1980, A&A 84, 60
Stenflo J.O., Twerenbold D., Harvey J.W., 1983a, A&AS 52, 161
Stenflo J.O., Twerenbold D., Harvey J.W., Brault J.W., 1983b, A&AS 54, 505
Vardavas I., 1976, J.Quant.Spectrosc.Radiat.Transfer 16, 715

This article was processed by the author using Springer-Verlag LaTeX A&A style file version 3.